Anomalous wave propagation in a one-dimensional acoustic metamaterial having simultaneously negative mass density and Young's modulus

H. H. Huang
Department of Engineering Science and Ocean Engineering, National Taiwan University, Taipei 10617, Taiwan

C. T. Sun[a)]
School of Aeronautics and Astronautics, Purdue University, West Lafayette, Indiana 47907

(Received 29 November 2011; revised 12 June 2012; accepted 21 July 2012)

A mechanical model representing an acoustic metamaterial that exhibits simultaneously negative mass density and negative Young's modulus was proposed. Wave propagation was studied in the frequency range of double negativity. In view of positive energy flow, it was found that the phase velocity in this range is negative. This phenomenon was also observed using transient wave propagation finite-element analyses of a transient sinusoidal wave and a transient wave packet. In contrast to wave propagation in the region of positive mass and modulus, the peculiar backward wave motion in the region of double negativity was clearly displayed.
 [http://dx.doi.org/10.1121/1.4744977]

PACS number(s): 43.35.Cg [ANN] Pages: 2887–2895

I. INTRODUCTION

For substances having simultaneously negative electric permittivity (ε) and magnetic permeability (μ), many unusual properties like reverse Doppler effect, reverse Cherenkov radiation, and negative index of refraction may arise.[1] The idea is that when both ε and μ are negative, the metamaterial may sustain waves with group velocity opposite to the phase velocity, and the waves can still propagate without attenuation.

Similar phenomena may apply to the counterpart acoustic metamaterials owing to the mathematical analogy between acoustic and electromagnetic waves. Theoretical or experimental attempts have been made for investigation of acoustic metamaterials possessing, for instance, negative effective mass density,[2–10] or negative effective elastic modulus,[11–13] or both simultaneously.[14–19] For metamaterials with double negativity, the consequence is the behavior of negative refraction, and, equivalently, negative phase-velocity and backward-wave phenomena.[1,20–22] Nevertheless, it has been shown that the negative refraction can be achieved not only by metamaterials with double negative properties, but also by Bragg scattering in periodic lattices[23] and others.[24,25] The similarity between these mechanisms relies on negative slope of dispersion curves in the first quadrant of dispersion relations.

According to the definition, the negative slope of the dispersion curve is related to negative group velocity. However, we agree with some references, e.g., Refs. 21 and 22, the term "negative phase velocity" is better for describing the negative slope of the dispersion curve than "negative group velocity," at least for the acoustic metamaterials with double negativity which is discussed in the present study. It also distinguishes the present metamaterials from the negative group-velocity media that exhibit fast-light phenomena reported in Refs. 26–29. It is noted that the subject of negative phase velocity has, surprisingly, been discussed since, at least, 1904 by Lamb,[30] using mechanical models, and by Schuster[31] in electromagnetism. At that time, the researchers were pessimistic about the physical applications.

The study of electromagnetic waves in anomalous dispersion has been extensively carried out by researchers in recent years, but that of acoustic and elastic waves receives much less attention. In the present study we propose a one-dimensional (1D) elastic mass-spring system consisting of material units exhibiting simultaneously negative effective mass density and effective elastic modulus in a spectral band. The local resonance acts as the central mechanisms of the unusual behavior. Transient wave propagation is simulated numerically to better observe the dynamic characteristics of negative phase velocity.

II. THEORETICAL MODELS OF ACOUSTIC METAMATERIALS

A. Model of negative mass density (NMD)

Let us begin with the mass-in-mass lattice model that has been discussed in Refs. 6–8. As illustrated in Fig. 1(a), the mass-in-mass unit takes the form of a rigid ring with mass, m_1, which is connected to the neighboring units by springs with spring constant, k_1. The ring contains an internal mass, m_2, connected to the ring by an internal spring with spring constant, k_2. Both m_1 and m_2 are only allowed to move in the x (horizontal) direction.

The equations of motion for the jth unit cell are given by

$$m_1\frac{d^2u_1^{(j)}}{dt^2}+k_1\left(2u_1^{(j)}-u_1^{(j-1)}-u_1^{(j+1)}\right)+k_2\left(u_1^{(j)}-u_2^{(j)}\right)=0, \quad (1)$$

a)Author to whom correspondence should be addressed. Electronic mail: sun@purdue.edu

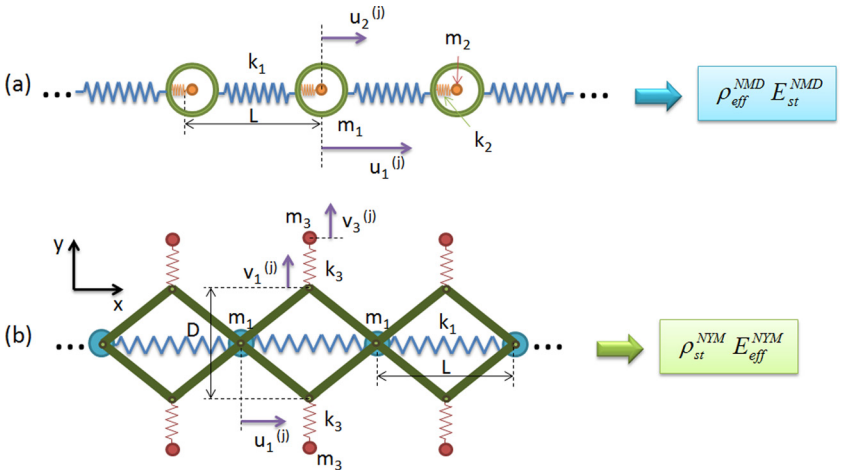

FIG. 1. (Color online) (a) 1D lattice model and the continuum representative having negative effective mass density (NMD), and (b) 1D lattice model and the continuum representative having negative effective Young's modulus (NYM).

$$m_2\frac{d^2u_2^{(j)}}{dt^2}+k_2\left(u_2^{(j)}-u_1^{(j)}\right)=0, \tag{2}$$

where $u_\gamma^{(j)}$ ($\gamma=1$ and 2) denotes the displacement of mass "γ" in the jth cell. The harmonic wave solution for the $(j+n)$th unit is expressed by

$$u_\gamma^{(j+n)}=\tilde{u}_\gamma e^{i(\xi X^*+n\xi-\eta T^*)}. \tag{3}$$

In Eq. (3), $\xi=qL$ is the non-dimensional wavenumber, $\eta=\omega/\omega_0^{\mathrm{NMD}}$ is the non-dimensional wave frequency, $\omega_0^{\mathrm{NMD}}=\sqrt{k_2/m_2}$ is the local resonance frequency, $X^*=x/L$ is the non-dimensional spatial parameter with the lattice spacing L, and $T^*=\omega_0^{\mathrm{NMD}}\cdot t$ is the non-dimensional time. The dispersion relation is obtained by substituting the harmonic displacements in Eq. (3) and solving the resulting eigenvalue problem of the coefficients. We obtain

$$\begin{aligned}G_{\mathrm{latt}}^{\mathrm{NMD}}(\eta=\omega/\omega_0^{\mathrm{NMD}},\xi=qL)&=\eta^4-\left[(1+\theta_{21})+\frac{2\theta_{21}}{\delta_{21}}(1-\cos\xi)\right]\eta^2\\&\quad+\frac{2\theta_{21}}{\delta_{21}}(1-\cos\xi)=0,\end{aligned} \tag{4}$$

where $\theta_{21}=m_2/m_1$ and $\delta_{21}=k_2/k_1$ are the non-dimensional mass ratio and stiffness ratio, respectively.

In Ref. 8, an effective elastic solid was developed to represent the original mass-in-mass lattice. It was found that the effective mass density of the equivalent elastic solid is frequency-dependent in the form

$$\rho_{\mathrm{eff}}^{\mathrm{NMD}}=\rho_{\mathrm{st}}^{\mathrm{NMD}}\left(1+\frac{\theta_{21}}{1+\theta_{21}}\frac{\eta^2}{1-\eta^2}\right), \tag{5}$$

where $\rho_{\mathrm{st}}^{\mathrm{NMD}}=(m_1+m_2)/AL$ is the static mass density in which A and L are the cross-sectional area and the lattice spacing, respectively. This model is denoted as "NMD" since it exhibits negative effective mass density in the range

$$1<\eta=\frac{\omega}{\omega_0^{\mathrm{NMD}}}<\sqrt{1+\theta_{21}}. \tag{6}$$

The time-independent wave equation for plane harmonic waves is simply given by

$$-\rho_{\mathrm{eff}}\omega^2\hat{u}=E_{\mathrm{eff}}\frac{\partial^2\hat{u}}{\partial x^2}, \tag{7}$$

where the effective mass density $\rho_{\mathrm{eff}}=\rho_{\mathrm{eff}}^{\mathrm{NMD}}$ is given in Eq. (5), and the effective Young's modulus, $E_{\mathrm{eff}}\equiv E_{\mathrm{st}}^{\mathrm{NMD}}\equiv k_1L/A$, is determined from the static stress-strain relation.

The harmonic wave solution for the equivalent elastic solid is given by $\hat{u}=\tilde{u}e^{i\xi X^*}$. Hence, the dispersion relation is obtained as

$$G_{\mathrm{elast}}^{\mathrm{NMD}}(\eta,\xi)=\rho_{\mathrm{eff}}^{\mathrm{NMD}}(\omega_0^{\mathrm{NMD}})^2\eta^2-E_{\mathrm{st}}^{\mathrm{NMD}}\xi^2/L^2=0. \tag{8}$$

B. Model of negative Young's modulus (NYM)

Next we consider the mechanical lattice model having lateral local resonators shown in Fig. 1(b). This model was investigated and discussed in Ref. 13. Briefly, point masses m_1 are connected by springs with a spring constant k_1. Four rigid and massless truss members are assembled symmetrically as shown to support two sets of microstructures consisting of springs with spring constant, k_3, and masses, m_3. Point mass m_3 is allowed to move only in the y (vertical) direction. L and D are geometrical parameters shown in Fig. 1(b).

For this lattice model, the equations of motion for the jth unit are given by

$$\begin{aligned}&m_1\frac{d^2u_1^{(j)}}{dt^2}+k_1\left(2u_1^{(j)}-u_1^{(j-1)}-u_1^{(j+1)}\right)\\&\quad+2k_3\left(v_3^{(j-1)}-v_1^{(j-1)}\right)\left(\frac{L}{2D}\right)\\&\quad-2k_3\left(v_3^{(j)}-v_1^{(j)}\right)\left(\frac{L}{2D}\right)=0,\end{aligned} \tag{9}$$

$$m_3\frac{d^2v_3^{(j)}}{dt^2}+k_3\left(v_3^{(j)}-v_1^{(j)}\right)=0. \tag{10}$$

From geometrical relations based on the assumption of small displacements, we have

$$\begin{aligned}v_1^{(j)}&=-\frac{(2L-\Delta u_1^{(j)})\Delta u_1^{(j)}}{4D}+\frac{(2L-\Delta u_1^{(j)})^2(\Delta u_1^{(j)})^2}{16D^3}+\cdots\\&\approx-\frac{L}{2D}\Delta u_1^{(j)}=-\frac{L}{2D}(u_1^{(j+1)}-u_1^{(j)}).\end{aligned} \tag{11}$$

In a similar manner, the dispersion relation is obtained as

$$G_{\text{latt}}^{\text{NYM}}(\bar{\eta}=\omega/\omega_0^{\text{NYM}},\xi=qL) = \bar{\eta}^4 - \left[1+\frac{2\theta_{31}}{\delta_{31}}\left(1+\frac{\delta_{31}\mu}{2}\right)(1-\cos\xi)\right]\bar{\eta}^2 + \frac{2\theta_{31}}{\delta_{31}}(1-\cos\xi)=0, \tag{12}$$

where $\theta_{31}=m_3/m_1$, $\delta_{31}=k_3/k_1$, $\bar{\eta}=\omega/\omega_0^{\text{NYM}}$, $\omega_0^{\text{NYM}}=\sqrt{k_3/m_3}$, and $\mu=(L/D)^2$. The relation of the non-dimensional wave frequencies reads

$$\bar{\eta}=\eta\sqrt{(\theta_{31}\delta_{21})/(\theta_{21}\delta_{31})}. \tag{13}$$

If this lattice system is represented by an equivalent elastic solid, the effective Young's modulus of the solid is found frequency-dependent in the form[13]

$$E_{\text{eff}}^{\text{NYM}}=E_{\text{st}}^{\text{NYM}}\left(1+\frac{\delta_{31}\mu}{2}\frac{\bar{\eta}^2}{\bar{\eta}^2-1}\right), \tag{14}$$

where $E_{\text{st}}^{\text{NYM}}=k_1L/A$ is the static Young's modulus. This model, denoted as "NYM," exhibits negative effective Young's modulus in the range

$$\sqrt{\frac{2}{2+\delta_{31}\mu}}<\bar{\eta}=\frac{\omega}{\omega_0^{\text{NYM}}}<1. \tag{15}$$

The wave equation takes the form of Eq. (7), in which the effective Young's modulus, $E_{\text{eff}}=E_{\text{eff}}^{\text{NYM}}$, is given by Eq. (14) and the effective mass density is the static formulation, $\rho_{\text{eff}}=\rho_{\text{st}}^{\text{NYM}}=m_1/AL$. (Note that the masses m_3 in this model are assumed to move only in the y direction so that they contribute zero inertia forces in the x direction.) The dispersion relation is given by

$$G_{\text{elast}}^{\text{NYM}}(\bar{\eta},\xi)=\rho_{\text{st}}^{\text{NYM}}(\omega_0^{\text{NYM}})^2\bar{\eta}^2-E_{\text{eff}}^{\text{NYM}}\xi^2/L^2=0. \tag{16}$$

C. Model of double negativity (DN)

Consider a 1D infinite lattice shown in Fig. 2. This model is a combination of the two models in Fig. 1 such that mass m_1 in the NYM model is replaced by the mass unit in NMD. This model is denoted as "DN" as it will be shown to possess double negativity. Let the displacements of masses m_1, m_2, and m_3 at the jth unit be $u_1^{(j)}(t)$, $u_2^{(j)}(t)$, $v_3^{(j)}(t)$, respectively. The equations of motion of the system at the jth cell are readily obtained as

$$m_1\frac{\partial^2u_1^{(j)}}{\partial t^2}=k_1(u_1^{(j-1)}-u_1^{(j)})+k_1(u_1^{(j+1)}-u_1^{(j)}) + k_2(u_2^{(j)}-u_1^{(j)})-2k_3(v_3^{(j-1)}-v_1^{(j-1)})\left(\frac{L}{2D}\right) + 2k_3(v_3^{(j)}-v_1^{(j)})\left(\frac{L}{2D}\right), \tag{17}$$

$$m_2\frac{\partial^2u_2^{(j)}}{\partial t^2}=k_2\left(u_1^{(j)}-u_2^{(j)}\right), \tag{18}$$

$$m_3\frac{\partial^2v_3^{(j)}}{\partial t^2}=k_3\left(v_1^{(j)}-v_3^{(j)}\right). \tag{19}$$

The steady-state solution of the equations of motion (17)–(19) is determined by letting the displacements be

$$u_1^{(j+n)}=\hat{u}_1e^{i(\xi X^*+n\xi-\eta T^*)},\quad u_2^{(j+n)}=\hat{u}_2e^{i(\xi X^*+n\xi-\eta T^*)},\ \text{and}\ v_3^{(j+n)}=\hat{v}_3e^{i(\xi X^*+n\xi-\eta T^*)}, \tag{20}$$

where, again, $\xi=qL$ is the non-dimensional wavenumber, $X^*=x/L$ and $T^*=\omega_0^{NMD}\cdot t$ are the non-dimensional parameters in space and time, respectively. Substituting these harmonic displacements in Eqs. (17)–(19) and solving the resulting eigenvalue problem of the coefficients, we obtain the dispersion relation

$$G_{\text{latt}}^{\text{DN}}(\eta,\xi)=-\eta^6+\left\{1+\frac{\delta_{31}\theta_{21}}{\delta_{21}\theta_{31}}+\frac{\theta_{21}}{\delta_{21}}\left[2\left(1+\frac{\delta_{31}\mu}{2}\right)(1-\cos\xi)+\delta_{21}\right]\right\}\eta^4 - \left[(1+\theta_{21})\frac{\delta_{31}\theta_{21}}{\delta_{21}\theta_{31}}+2\frac{\theta_{21}}{\delta_{21}}\left(\frac{\delta_{31}\theta_{21}}{\delta_{21}\theta_{31}}+1+\frac{\delta_{31}\mu}{2}\right)(1-\cos\xi)\right]\eta^2+2\frac{\delta_{31}\theta_{21}^2}{\delta_{21}^2\theta_{31}}(1-\cos\xi)=0. \tag{21}$$

On the other hand, the equation of motion of the equivalent 1D elastic solid is given by Eq. (7). In this formulation the effective mass density and the effective Young's modulus are given by Eq. (5), $\rho_{\text{eff}}=\rho_{\text{eff}}^{\text{DN}}=\rho_{\text{eff}}^{\text{NMD}}$, and Eq. (14), $E_{\text{eff}}=E_{\text{eff}}^{\text{DN}}=E_{\text{eff}}^{\text{NYM}}$, respectively. Consequently, the dispersion relation of the representative elastic solid is obtained as

$$G_{\text{elast}}^{\text{DN}}(\eta,\xi)=\rho_{\text{eff}}^{\text{DN}}(\omega_0^{\text{NMD}})^2\eta^2-E_{\text{eff}}^{\text{DN}}\xi^2/L^2=0. \tag{22}$$

III. EFFECTIVE DYNAMIC PARAMETERS AND DISPERSION RELATION

For numerical illustrations, we present two cases with the following assumed material constants:

(Case 1) $\theta_{21}=m_2/m_1=1.5$, $\theta_{31}=m_3/m_1=1$, $\delta_{21}=k_2/k_1=0.1$, $\delta_{31}=k_3/k_1=1$, $\mu=(L/D)^2=2.78$,

and

(Case 2) $\theta_{21}=2.25$, $\theta_{31}=0.4$, $\delta_{21}=0.3$, $\delta_{31}=0.25$, $\mu=25$.

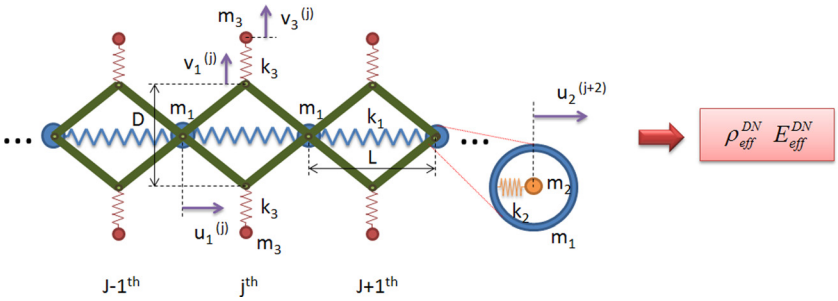

FIG. 2. (Color online) One-dimensional lattice model exhibiting DN.

As has been mentioned in Sec. II C, the model in Fig. 2 is denoted as "DN" because for some range of wave frequencies it could exhibit double negativity. This range can be obtained from the negative modulus and mass density properties and their corresponding spectral regions. The effective mass density in Eq. (5) and the effective Young's modulus in Eq. (14) with respect to the non-dimensional wave frequency for Case 1 and Case 2 are illustrated in Figs. 3 and 4, respectively.

In Fig. 3 for Case 1, the material constants are selected so that the frequency range of the negative quantity of the NMD model lies apart from that of the NYM model. In other words, for the frequency range in-between the two regions with negative quantity (e.g., η approximately ranges in 1.6 and 2.5 in Fig. 3), both the effective mass density and the effective Young's modulus are positive. On the other hand, in Fig. 4 for Case 2, the material constants are chosen so that the frequency ranges of both negative quantities of the NMD and the NYM models overlap.

Next, the dispersion curves for both cases obtained using the exact formulation [Eqs. (4), (12), and (21) for NMD, NYM, and DN models, respectively] of the lattice model are shown in Figs. 5 and 6, respectively, with solid lines. In each figure, three columns labeled DN, NMD, and NYM represent the dispersion curves of the double negativity model, the negative mass density model, and the negative Young's modulus model, respectively. For each diagram, bandgaps, where waves attenuated and stopped, exist due to the effect of the local resonance.

The accuracy of the elastic solid representation can be verified by comparing the dispersion curves obtained with the lattice and the elastic solid models. In Figs. 5 and 6, the dispersion curves of the equivalent elastic solid are obtained using Eqs. (8), (16), and (22) for the NMD, NYM, and DN models, respectively. Good approximation is observed for the lower branch for all models. For the higher branch some deviation is seen at the high frequency range. The reason is that the equivalent elastic solid employs an approximate formulation from the original lattice system based on a long wavelength approximation. It is noted that the shaded areas in the figures indicate the negative properties derived from Eqs. (6) and (15) for the NMD and NYM model, respectively. For both cases and for the DN model, the bandgaps closely match the shaded areas of the separate models.

IV. PHASE VELOCITY AND GROUP VELOCITY

A. Phase velocity

In the present study, we adopt the definition of the phase velocity of a harmonic wave as[32–34]

$$v_p = \frac{\omega}{q}. \tag{23}$$

All points of the same phase propagate in space with this velocity. In the dispersion ω-q diagram, the phase velocity

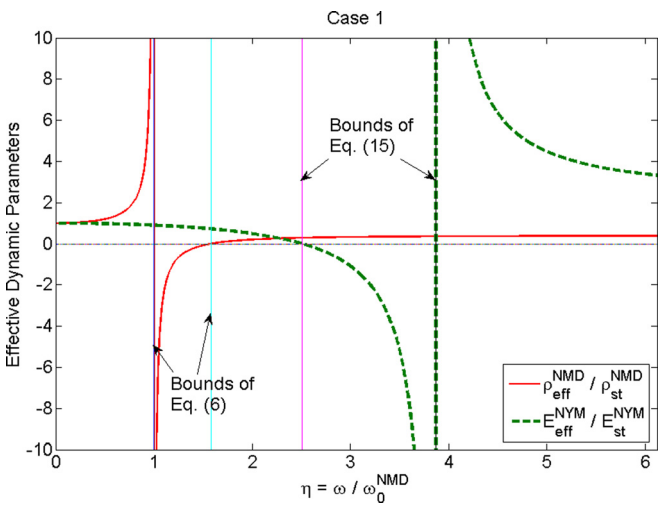

FIG. 3. (Color online) Effective dynamic non-dimensional parameters for Case 1 using Eqs. (5) and (14). The bounds of negative quantities are described in Eqs. (6) and (15).

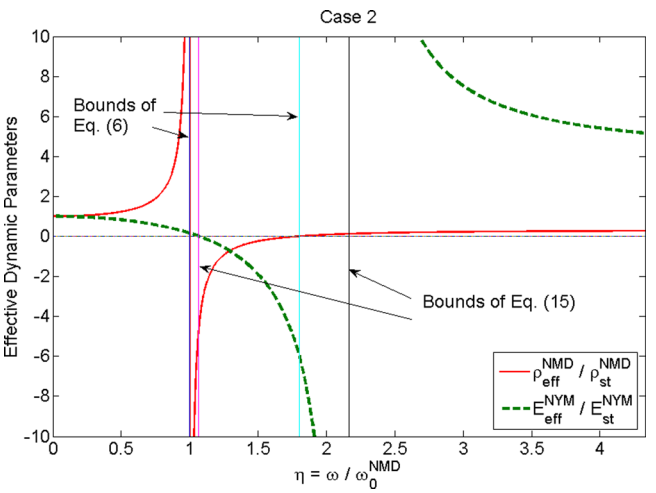

FIG. 4. (Color online) Effective dynamic non-dimensional parameters for Case 2. Descriptions as in Fig. 3.

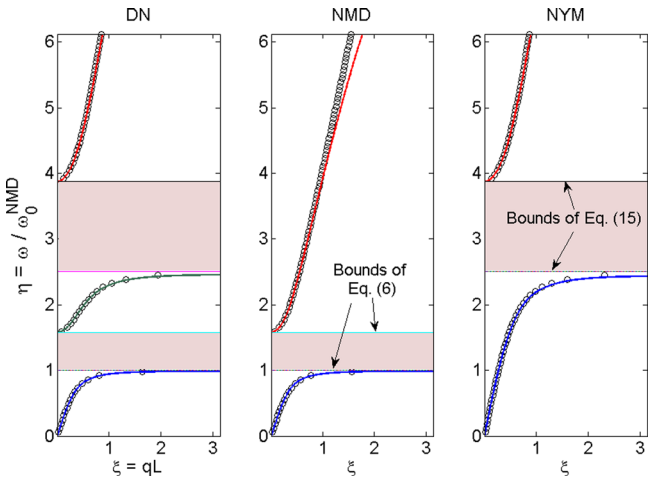

FIG. 5. (Color online) Dispersion curves for Case 1. DN model, NMD model, NYM model; solid lines: mass-spring lattice model from Eqs. (4), (12), and (21) for NMD, NYM, and DN models, respectively; circles: equivalent elastic solid from Eqs. (8), (16), and (22) for NMD, NYM, and DN models, respectively.

is given by the slope of the straight line connecting the origin and a certain point on the dispersion curve. Since negative wave frequency is not in our consideration, it is obvious that the wave vector, $\vec{q}$, points in the direction of phase velocity.

For an effective elastic solid of an acoustic metamaterial, the dispersion relation can be obtained by, for instance, employing Eq. (7) together with ρ_{eff} in Eq. (5) and E_{eff} in Eq. (14), and substituting the harmonic plane-wave solution into Eq. (7). The dispersion relation reads

$$G(\omega, q) = \rho_{\text{eff}}\omega^2 - E_{\text{eff}}q^2 = 0. \tag{24}$$

From the dispersion relation, one can immediately conclude that in order for the elastic medium to have wave propagation without attenuation (i.e., a real solution for q), the medium must have either both positive ρ_{eff} and E_{eff} or both negative ρ_{eff} and E_{eff}.

The phase velocity is thus given by

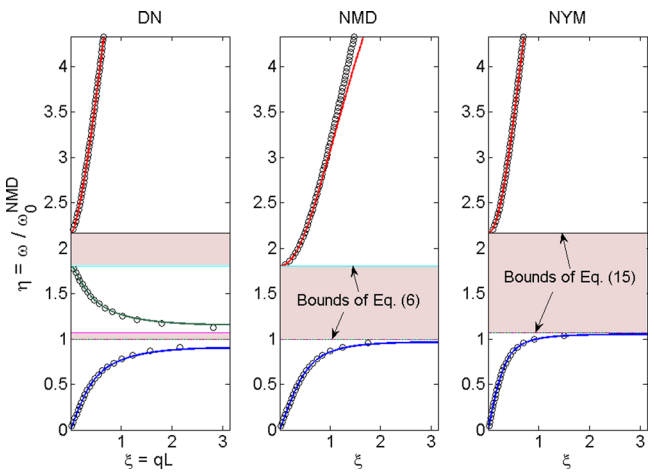

FIG. 6. (Color online) Dispersion curves for Case 2. Solid lines: mass-spring lattice model; Circles: elastic solid model; detailed description as in Fig. 5.

$$v_p = \frac{\omega}{q} = \pm\sqrt{\frac{E_{\text{eff}}}{\rho_{\text{eff}}}}. \tag{25}$$

It is still not possible to determine the direction of a wave in the acoustic metamaterial from the sign of phase velocity, or the wave vector, based on the given dispersion relation, since the real wave vector q could be either positive or negative. We shall proceed to the next subsections for further investigation.

B. Group velocity of DN acoustic metamaterial

Of particular interest is to investigate the sign of group velocity of a wave group or packet in an acoustic metamaterial. This wave group or packet corresponds to a superposition of harmonic waves with very similar wave frequencies, ω, and wavenumbers, q. In the dispersion ω-q diagram, the group velocity of a wave group or packet is given by the slope of the dispersion curve. By using the implicit differentiation, the final expression of the group velocity reads

$$v_g = \frac{d\omega}{dq} = -\left(\frac{\partial G}{\partial \omega}\right)^{-1}\left(\frac{\partial G}{\partial q}\right) = \frac{2E_{\text{eff}}q}{2\rho_{\text{eff}}\omega + \left(\frac{\partial \rho_{\text{eff}}}{\partial \omega} - \frac{\partial E_{\text{eff}}}{\partial \omega}\frac{\rho_{\text{eff}}}{E_{\text{eff}}}\right)\omega^2}. \tag{26}$$

From the expressions given by Eqs. (5) and (14), it can be shown that

$$\frac{\partial \rho_{\text{eff}}}{\partial \omega} = \frac{2\rho_{\text{st}}^{\text{NMD}}\lambda}{\omega_0^{\text{NMD}}}\frac{\eta}{(1-\eta^2)^2} \geq 0 \tag{27}$$

and

$$\frac{\partial E_{\text{eff}}}{\partial \omega} = -\frac{E_{\text{st}}^{\text{NYM}}\delta_{31}\mu}{\omega_0^{\text{NYM}}}\frac{\bar{\eta}}{(\bar{\eta}^2-1)^2} \leq 0, \tag{28}$$

where $\lambda = \theta_{21}/(1+\theta_{21})$. The term $[-(\partial E_{\text{eff}}/\partial\omega)(\rho_{\text{eff}}/E_{\text{eff}})]\omega^2$ in the denominator in Eq. (26) is always positive if ρ_{eff} and E_{eff} are of the same sign. Substituting Eqs. (5) and (26) in the remainder of the denominator of Eq. (26), $2\rho_{\text{eff}}\omega + (\partial\rho_{\text{eff}}/\partial\omega)\omega^2$, we obtain

$$2\rho_{\text{eff}}\omega + \left(\frac{\partial \rho_{\text{eff}}}{\partial \omega}\right)\omega^2 = \frac{2\rho_{\text{st}}^{\text{NMD}}\omega}{(1-\eta^2)^2}[(1-\lambda)(1-\eta^2)^2 + \lambda] \geq 0. \tag{29}$$

Since $0 \leq \lambda \leq 1$ is always true, this inequality holds for all frequencies. It is, therefore, proved that the denominator of Eq. (26) is positive for identical signs of ρ_{eff} and E_{eff}.

Obviously, from Eq. (26), group velocity, v_g, is proportional to $E_{\text{eff}}q$. The sign of group velocity is, hence, affected by the sign of the effective Young's modulus, E_{eff}, and the wavenumber, q. From Sec. IV A, in order for an elastic medium to have wave propagation without attenuation, the medium must possess either both positive ρ_{eff} and E_{eff} or both

negative ρ_{eff} and E_{eff}. If ρ_{eff} and E_{eff} of the medium are both positive, group velocity, v_g, is obviously positive for a positive wavenumber. On the other hand, if ρ_{eff} and E_{eff} are simultaneously negative, waves, therefore, propagate in the medium with opposite signs of phase velocity, v_p, and group velocity, v_g.

C. Negative phase velocity

For waves in a lossless elastic medium the energy velocity is identical to the group velocity.[35] In view of positive energy flow for a lossless elastic medium, the group velocity is always positive. Once again, we exclude the negative group-velocity media resulting in fast-light phenomena discussed in, for instance, Refs. 26–29. That negative group-velocity phenomenon is beyond the scope of the present study.

For the acoustic metamaterial with frequency-dependent effective mass density, ρ_{eff}, and Young's modulus, E_{eff}, if ρ_{eff} and E_{eff} are both positive, a positive group velocity results in a positive wavenumber. On the other hand, ifρ_{eff} and E_{eff} are negative simultaneously, in order to have a positive group velocity, wavenumber must be negative. This means that in the double negativity frequency region, the sign of phase velocity, v_p, in Eq. (25) must be negative.

V. DYNAMIC CHARACTERISTICS OF WAVE PROPAGATION BY SIMULATION

A. Harmonic waves

To investigate how a group of waves of essentially the same wavelength propagates with a negative phase velocity, we perform numerical simulations of transient wave propagations. One of the reasons the transient wave propagation rather than steady-state wave propagation is studied is because the direction of disturbances, hence the direction of group velocity, can be ensured.

Dynamic simulations are implemented by use of the ABAQUS Explicit solver (Dassault Systèmes, Vèlizy-Villacoublay, France). In each simulation, a lattice model shown in Fig. 2 is constructed with a sinusoidal displacement, $U(t) = U_0 \sin(\omega t) H(t)$, applied at the left end of the lattice. The material properties of Case 2 listed in Sec. III together with $\omega_0^{\text{NMD}} = 115.47$ rad/s are used. If the lattice system is long enough, the reflected wave does not appear in the window of numerical results.

Figures 7 and 8 show the snapshots of the displacement fields in space with two different wave frequencies, $\eta = \omega/\omega_0^{\text{NMD}} = 0.346$ and 1.559, respectively. U^* denotes the normalized amplitude of the displacements with respect to U_0. In each figure, a typical propagation mode is demonstrated. Three consecutive sections of time, $T^* = \text{ts} \cdot \Delta T^*$ with the non-dimensional time increment $\Delta T^* = 0.462$, show the behavior of wave propagation. For now, let us assume that the time increment ΔT^* is sufficiently small in capturing the dynamic behavior of the model. We shall come to this point immediately in the following paragraph. Note that, again, $T^* = \omega_0^{\text{NMD}} \cdot t$ is the non-dimensional parameter in time domain and t is in seconds. "ts" denotes

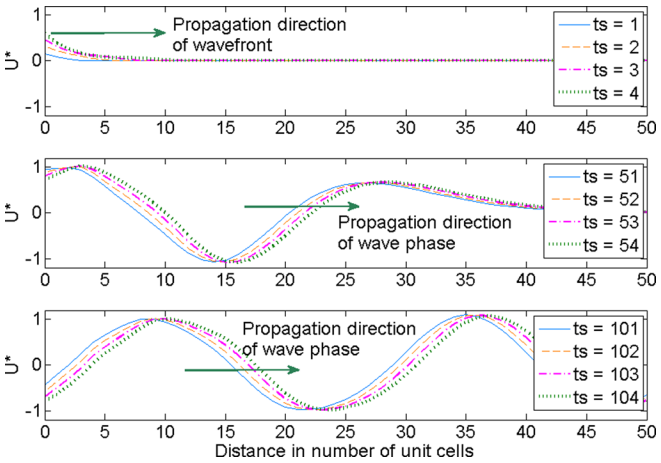

FIG. 7. (Color online) Snapshots of sinusoidal wave propagation in finite DN model with excitation frequency $\eta = \omega/\omega_0^{\text{NMD}} = 0.346$ and $\omega_0^{\text{NMD}} = 115.47$ rad/s (in the double-positivity region; ts = time step; $T^* = \omega_0^{\text{NMD}} \cdot t = \text{ts} \cdot \Delta T^*$ with $\Delta T^* = 0.462$).

the time steps hereafter. Section 1 (ts = 1–4), for instance, is the initial state and section 3 (ts = 101–104) is considered close to steady state.

Selection of the time increment, ΔT^*, for visualization of simulation results is nontrivial. An improper selection of the increments may, on one hand, produce incorrect simulation results, or, on the other hand, simply cause expensive computation. Here we provide a simple guide for the balance of accuracy and efficiency. The definition of the time increment reads

$$\Delta T^* = \omega_0^{\text{NMD}} \frac{t}{\text{ts}} = \omega_0^{\text{NMD}} \cdot \Delta t, \tag{30}$$

where Δt is the time step in seconds. Substituting the non-dimensional wave frequency $\eta = \omega/\omega_0^{\text{NMD}}$ in Eq. (30) and using the relationship of angular frequency and period of time we obtain

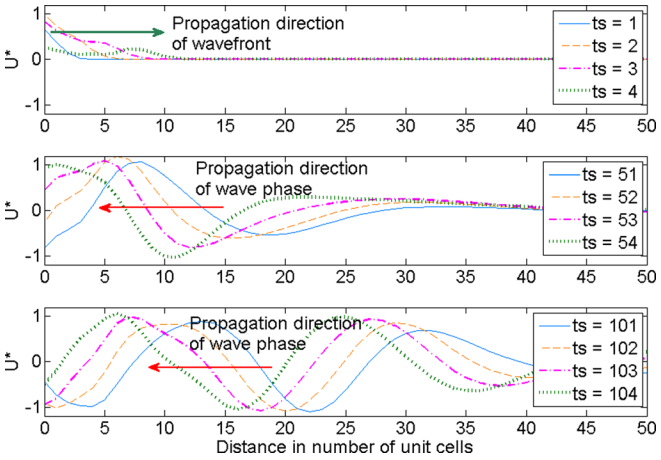

FIG. 8. (Color online) Snapshots of sinusoidal wave propagation in finite DN model with excitation frequency $\eta = \omega/\omega_0^{\text{NMD}} = 1.559$ and $\omega_0^{\text{NMD}} = 115.47$ rad/s (in the double-negativity region; ts = time step; $T^* = \omega_0^{\text{NMD}} \cdot t = \text{ts} \cdot \Delta T^*$ with $\Delta T^* = 0.462$).

$$\Delta T^* = \frac{2\pi}{\eta}\frac{\Delta t}{T_p}. \tag{31}$$

For a harmonic wave, $\Delta t \leq T_p/8$ should be sufficient in capturing the dynamic behavior of the models in the present study. For Case 2, for instance, this inequality $\Delta t \leq T_p/8$ and the wave frequency, $\eta = 1.559$, together with Eq. (31), result in $\Delta T^* \leq 0.504$. Clearly, the time increments chosen for both cases are satisfactory.

In Fig. 7, given the first section from ts = 1–4, the propagation direction of the front of the dynamic disturbance is seen pointing from left to right, indicating the direction of the energy flow. However, due to the nature of transient wave propagation, the forerunner of the dynamic disturbance may contain frequencies other than the excitation frequency, ω. Further time steps, in the middle and bottom windows of Fig. 7, need to be carried out in order to make sure the energy direction of the sinusoidal wave with exactly the excitation frequency, ω. In the second section, ts = 51–54, it is seen that the transient part of the wave already propagates to the right side of the spatial window, leaving the transition to steady state at the left part of the window. From the third section, ts = 101–104, a more complete configuration approaching the steady-state wave propagation can be observed. At this stage, the propagation direction of the wave phase is observed pointing from left to right.

Figure 8 shows the profile of wave propagation with a frequency in the region of double negativity. Noticeable difference to Fig. 7 is the negative propagation direction of the wave phase with respect to positive energy flow. In the second and third windows, the phase direction is clearly seen pointing from right to left during the sequence of time evolution.

B. Wave packets

Group velocity is the velocity of the envelope of a wave group or packet. For a wave packet corresponding to a superposition of harmonic waves with a finite frequency band, the propagation behavior in a dispersive media like DN acoustic metamaterial should be of particular interest. One great advantage of considering the wave packet is that the frequency content of the packet can be controlled and the energy propagation direction can be easily identified as the propagation direction of the wave packet.

To this end, wave packets propagating in the metamaterial with double negativity are simulated in a similar fashion. Two wave packets in time as well as in frequency domain used for the simulation are illustrated in Fig. 9. In Fig. 9(a), the wave packet possesses a frequency band approximately from $\eta = \omega/\omega_0^{\mathrm{NMD}} = 0.22$ to $\eta = 0.47$ (in the double positivity region) with the central frequency at $\eta = 0.346$, while in Fig. 9(b), the wave packet possesses a frequency band approximately from $\eta = \omega/\omega_0^{\mathrm{NMD}} = 1.10$ to $\eta = 2.10$ (in the double negativity region) with the central frequency at $\eta = 1.559$. Each packet is sent from the left end of the model. Same material properties are chosen so that the dispersion relation of the model is shown in Fig. 6.

Figure 10 shows a few snapshots of wave propagation of the wave packet shown in Fig. 9(a), of which the central frequency is located at the positive effective mass density and positive effective elastic modulus region as shown in Fig. 4. The wave packet propagates without much distortion since most of the spectral content travel with approximately the same speed, which is also evident in view of the dispersion curves shown in Fig. 6. The energy flow direction is the moving direction of the wave packet, which is clearly from left to right. Note that a wave packet contains not just a single frequency,

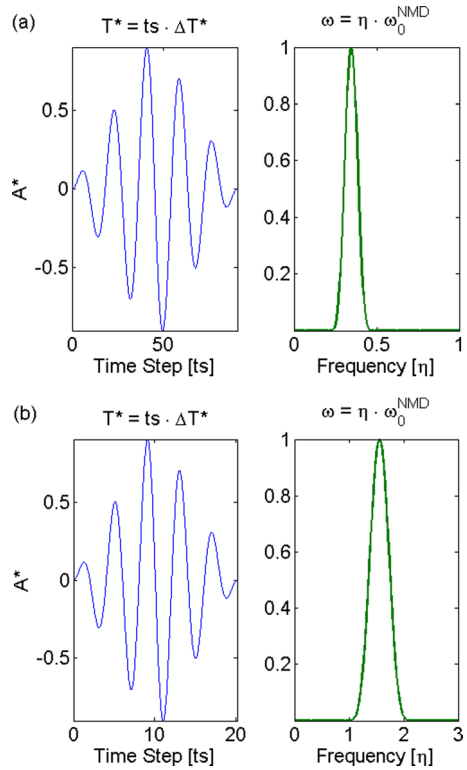

FIG. 9. (Color online) Two typical wave packets in time and frequency domain with (a) frequency band approximately from $\eta = \omega/\omega_0^{\mathrm{NMD}} = 0.22$ to $\eta = 0.47$ with the central frequency at $\eta = 0.346$, and (b) frequency band approximately from $\eta = \omega/\omega_0^{\mathrm{NMD}} = 1.10$ to $\eta = 2.10$ with the central frequency at $\eta = 1.559$.

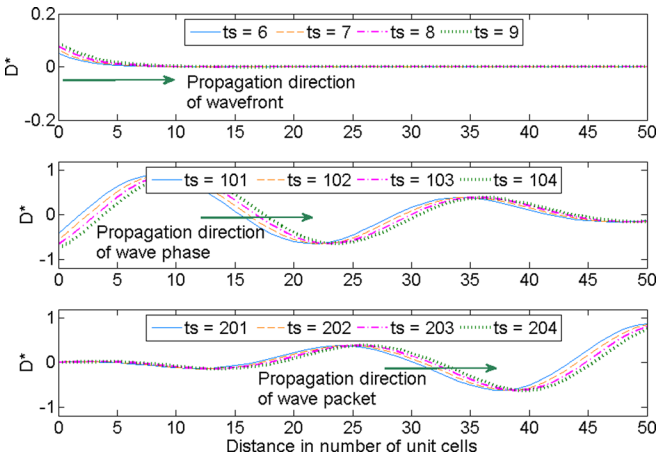

FIG. 10. (Color online) Snapshots of wave-packet propagation in finite DN model. Wave packet consists of frequency band approximately from $\eta = \omega/\omega_0^{\mathrm{NMD}} = 0.22$ to $\eta = 0.47$ with the central frequency at $\eta = 0.346$ and $\omega_0^{\mathrm{NMD}} = 115.47$ rad/s (in the double-positivity region; ts = time step; $T^* = \omega_0^{\mathrm{NMD}} \cdot t = \mathrm{ts} \cdot \Delta T^*$ with $\Delta T^* = 0.462$).

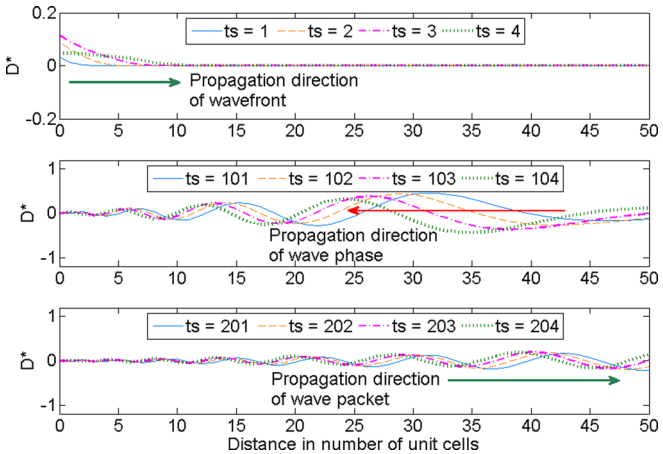

FIG. 11. (Color online) Snapshots of wave-packet propagation in the DN model. Wave packet consists of frequency band approximately from $\eta = \omega/\omega_0^{\mathrm{NMD}} = 1.10$ to $\eta = 2.10$ with the central frequency at $\eta = 1.559$ and $\omega_0^{\mathrm{NMD}} = 115.47$ rad/s (in the double-negativity region; ts = time step; $T^* = \omega_0^{\mathrm{NMD}} \cdot t = \mathrm{ts} \cdot \Delta T^*$ with $\Delta T^* = 0.462$).

but a finite frequency band. It is therefore difficult to identify the phase velocity of the propagation of the wave packet.

Next, consider the case when the frequency components of the wave packet are selected in the frequency region of double negativity. A wave packet of Fig. 9(b) is generated for simulation. The frequency band of this wave packet is inside the double negativity region shown in Fig. 4. The wave packet is sent from the left end and is clearly seen to propagate in the positive direction (left to right) from the top and bottom windows of Fig. 11. Negative phase direction of the packet is expected and can be verified from the middle window of Fig. 11.

C. Discussion

The region of the dispersion curve with negative slope means a spectral range where the phase and group velocities are opposite in direction. Some researchers[25,30,36–38] have termed the backward-wave phenomenon along with "negative group velocity" simply because, perhaps, in the ω-q diagram

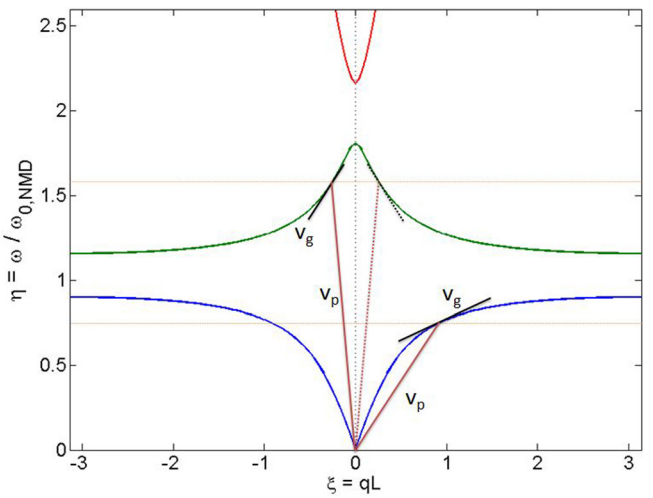

FIG. 12. (Color online) Schematic of group velocity and phase velocity in ω-q diagram.

the slope of the dispersion curve is negative. For example, let us refer to the dispersion diagram in Fig. 12 for illustration. The dispersion curves are reproduced from Fig. 6, Case 2 in Sec. V, for the DN model. Usually the first quadrant of the diagram is considered where ω and q are both positive. For the first lowest propagation mode, both phase velocity and group velocity, according to the definition in Sec. IV, are positive. However, for the second lowest propagation mode in the first quadrant, the phase velocity is positive while the group velocity is negative. The misleading and confusing conclusion of the "negative group velocity" may have come from the fact that energy velocity is not directly provided by the dispersion curves in the first quadrant. In fact, the second branch of the dispersion curve should be plotted in the second quadrant where ω is positive and q is negative. By so doing, the group velocity is positive while the phase velocity is, hence, negative.

VI. CONCLUSION

We have proposed a 1D mechanical model representing an acoustic metamaterial. The system can be modeled with an equivalent elastic solid which exhibits simultaneously negative effective mass density and effective Young's modulus in a certain frequency range. In this double negativity frequency range, harmonic waves propagate without attenuation. However, the phase velocity becomes opposite to the energy flow direction. In view of positive energy direction, it is the backward wave that propagates with negative phase velocity. Transient wave simulation results not only agree well with the analytical prediction, but also clearly illustrate the unusual wave phenomenon.

ACKNOWLEDGMENT

This work was supported by an AFOSR Grant No. FA9550-10-1-0061. Dr. Les Lee was the program manager.

[1]V. G. Veselago, "The electrodynamics of substances with simultaneously negative values of ε and μ," Sov. Phys. Usp. **10**, 509–514 (1968).
[2]Z. Liu, X. Zhang, Y. Mao, Y. Y. Zhu, Z. Yang, C. T. Chan, and P. Sheng, "Locally resonant sonic materials," Science **289**, 1734–1736 (2000).
[3]Z. Liu, C. T. Chan, and P. Sheng, "Analytic model of phononic crystals with local resonances," Phys. Rev. B **71**, 014103 (2005).
[4]G. W. Milton and J. R. Willis, "On modifications of Newton's second law and linear continuum elastodynamics," Proc. R. Soc. London, Ser. A **463**, 855–880 (2007).
[5]S. Yao, X. Zhou, and G. Hu, "Experimental study on negative mass effective mass in a 1D mass-spring system," New J. Phys. **10**, 043020 (2008).
[6]H. H. Huang, C. T. Sun, and G. L. Huang, "On the negative effective mass density in acoustic metamaterials," Int. J. Eng. Sci. **47**, 610–617 (2009).
[7]H. H. Huang and C. T. Sun, "Wave attenuation mechanism in an acoustic metamaterial with negative effective mass density," New J. Phys. **11**, 013003 (2009).
[8]H. H. Huang and C. T. Sun, "Locally resonant acoustic metamaterials with 2D anisotropic effective mass density," Philos. Mag. **91**, 981–996 (2011).
[9]S. H. Lee, C. M. Park, Y. M. Seo, Z. G. Wang, and C. K. Kim, "Acoustic metamaterial with negative density," Phys. Lett. A **373**, 4464–4469 (2009).
[10]M. T. Islam and G. Newaz, "Metamaterial with mass-stem array in acoustic cavity," Appl. Phys. Lett. **100**, 011904 (2012).
[11]N. Fang, D. Xi, J. Xu, M. Ambati, W. Srituravanich, C. Sun, and X. Zhang, "Ultrasonic metamaterials with negative modulus," Nature Mater. **5**, 452–456 (2006).

[12]S. H. Lee, C. M. Park, Y. M. Seo, Z. G. Wang, and C. K. Kim, "Acoustic metamaterial with negative modulus," J. Phys. Condens. Matter **21**, 175504 (2009).
[13]H. H. Huang and C. T. Sun, "Theoretical investigation of the behavior of an acoustic metamaterial with extreme Young's moduli," J. Mech. Phys. Solids **59**, 2070–2081 (2011).
[14]J. Li and C. T. Chan, "Double-negative acoustic metamaterial," Phys. Rev. E **70**, 055602 (2004).
[15]Y. Ding, Z. Liu, C. Qiu, and J. Shi, "Metamaterial with simultaneously negative bulk modulus and mass density," Phys. Rev. Lett. **99**, 093904 (2007).
[16]Y. Cheng, J. Y. Xu, and X. J. Liu, "One-dimensional structured ultrasonic metamaterials with simultaneously negative dynamic density and modulus," Phys. Rev. B **77**, 045134 (2008).
[17]S. H. Lee, C. M. Park, Y. M. Seo, Z. G. Wang, and C. K. Kim, "Composite acoustic medium with simultaneously negative density and modulus," Phys. Rev. Lett. **104**, 054301 (2010).
[18]L. Fok and X. Zhang, "Negative acoustic index metamaterial," Phys. Rev. B **83**, 214304 (2011).
[19]G. K. Hu, G. L. Huang, and C. T. Sun, "An elastic metamaterial with simultaneously negative mass density and bulk modulus," Appl. Phys. Lett. **98**, 251907 (2011).
[20]I. V. Lindell, S. A. Tretyakov, K. I. Nikoskinen, and S. Ilvonen, "BW media—Media with negative parameters, capable of supporting backward waves," Microwave Opt. Technol. Lett. **31**, 129–133 (2001).
[21]A. Lakhtakia, M. W. McCall, and W. S. Weiglhofer, "Brief overview of recent developments on negative phase-velocity mediums (alias left-handed materials)," AEU, Int. J. Electron. Commun. **56**, 407–410 (2002).
[22]K. Aydin and K. Guven, "Observation of negative refraction and negative phase velocity in left-handed metamaterials," Appl. Phys. Lett. **86**, 124102 (2005).
[23]M. Notomi, "Theory of light propagation in strongly modulated photonic crystals: Refractionlike behavior in the vicinity of the photonic band gap," Phys. Rev. B **62**, 10696–10705 (2000).
[24]H. Chen, K. H. Fung, H. Ma, and C. T. Chan, "Polarization gaps and negative group velocity in chiral phononic crystals: Layer multiple scattering method," Phys. Rev. B **77**, 224304 (2008).
[25]X. Ao and C. T. Chan, "Negative group velocity from resonances in two-dimensional phononic crystals," Waves Random Complex Media **20**, 276–288 (2010).
[26]L. J. Wang, A. Kuzmich, and A. Dogariu, "Gain-assisted superluminal light propagation," Nature **406**, 277–279 (2000).
[27]R. W. Boyd and D. J. Gauthier, " 'Slow' and 'fast' light," Prog. Opt. **43**, 497–530 (2002).
[28]E. Feigenbaum, N. Kaminski, and M. Orenstein, "Negative dispersion: A backward wave or fast light? Nanoplasmonic examples," Opt. Express **17**, 18934 (2009).
[29]R. W. Boyd and D. J. Gauthier, "Controlling the velocity of light pulses," Science **326**, 1074–1077 (2009).
[30]H. Lamb, "On group-velocity," Proc. London Math. Soc. **1**, 473–479 (1904).
[31]A. Schuster, *An Introduction to the Theory of Optics* (Arnold, London, 1904), Chap. XIII, pp. 297–318.
[32]L. Brillouin, *Wave Propagation and Group Velocity* (Academic, New York, 1960), pp. 1–154.
[33]A. Hirose and K. E. Lonngren, *Introduction to Wave Phenomena* (Wiley-Interscience, New York, 1985), Chap. 2.6, pp. 40–43.
[34]F. K. Kneubühl, *Oscillations and Waves* (Springer, Berlin, 1997), Chap. 7.3, pp. 356–368.
[35]L. Brillouin, *Wave Propagation in Periodic Structures* (Dover, New York, 1953), Chap, V, pp. 69–93.
[36]P. L. Marston, "Negative group velocity Lamb waves on plates and applications to the scattering of sound by shells," J. Acoust. Soc. Am. **113**, 2659–2662 (2003).
[37]G. Monti and L. Tarricone, "Negative group velocity in a split ring resonator-coupled microstrip line," PIER **94**, 33–47 (2009).
[38]M. I. Shalaev, S. A. Myslivets, V. V. Slabko, and A. K. Popov, "Negative group velocity and three-wave mixing in dielectric crystals," Opt. Lett. **36**, 3861–3863 (2011).